The Visual Hull of Curved Objects

Aldo Laurentini, *member, IEEE*

Dipartimento di Automatica ed Informatica,Politecnico di Torino,
Corso Duca degli Abruzzi 24, 10129 Torino, Italy
laurentini@polito.it

Abstract. The visual hull is a geometric tool which relates the 3D shape of a concave object to its silhouettes or shadows. This paper develops the theory of the visual hull of objects bounded by smooth curved surfaces. From the basic definitions of visual hull we determine the surfaces which bound the visual hull of such objects. We show that these surfaces are patches of some surfaces which partition the viewpoint space of the aspect graph of the object. The surfaces concerned are those generated by the visual events *tangent crossing* and *triple point.* These ruled surfaces are analyzed for finding their active parts, i.e. the parts which could actually bound the visual hull. This analysis is based on the shape of the surface of the object at the tangency points of the ruled surfaces. An algorithm for computing the visual hull of a smooth curved object is outlined, which exploits the algorithm for computing its aspect graph .

Index Terms. Computer vision, aspect, aspect graphs, silhouettes, visual hull

1. INTRODUCTION

This paper addresses the problem of finding the visual hull of concave objects bounded by smooth curved surfaces. We will show that the visual hull of a such object is related with its aspect graph. In fact, we have found that the surface of the visual hull that bounds concavities of the object consists of sub-patches of two surfaces used for partitioning the viewing space of the aspect graph.

These surfaces, related to two particular visual events, are generated by lines tangent at two or three points of the object.

We will also present a detailed analysis, based on the geometry of the curved object at the tangency points, for determining in which cases these ruled surfaces can actually bound the visual hull, and which parts of the surface are relevant. Finding these potential boundaries of the visual hull can be done exploiting the algorithms for computing the aspect graph. An algorithm for computing the visual hull from the potential boundaries will be also outlined.

In the rest of this section we overview the basic concepts of visual hull and aspect graph.

The visual hull is a geometric entity useful for comparing or understanding the shape of 3D objects using their silhouettes or shadows[9]. The visual hull **VH**(**O**,**VR**) of an object **O** relative to a viewing region **VR** of $\boldsymbol{R}^3$ is the largest object that produces the same silhouettes (or shadows) as **O** observed from viewpoints (lighted from point lights) belonging to **VR**. The visual hull is also the closest approximation of **O** which can be obtained from silhouettes (or shadows) with viewpoints (or point light sources) belonging to **VR**.

All the visual hulls relative to viewing regions which: 1) completely enclose **O**; 2) do not share any point with the convex hull of **O**; are equal. This is the external visual hull of **O**, or simply the visual hull **VH**(**O**). If the viewing region is bounded by the object **O** itself, we have the internal visual hull **IVH**(**O**). The external visual hull is relevant to most practical situations.

Visual hull, internal visual hull and convex hull **CH**(**O**)are related by the following inequalities: **IVH**(**O**)≤ **VH**(**O**) ≤ **CH**(**O**). For convex objects, all these entities are coincident.

An intuitive physical construction of the visual hull of a concave object is as follows. Suppose filling the concavities of the object with soft material. The visual hull can be obtained by scraping off the excess material with a ruler grazing the hard surface of the object in all possible ways (see Fig.1, where **O** is one half of an object of revolution)

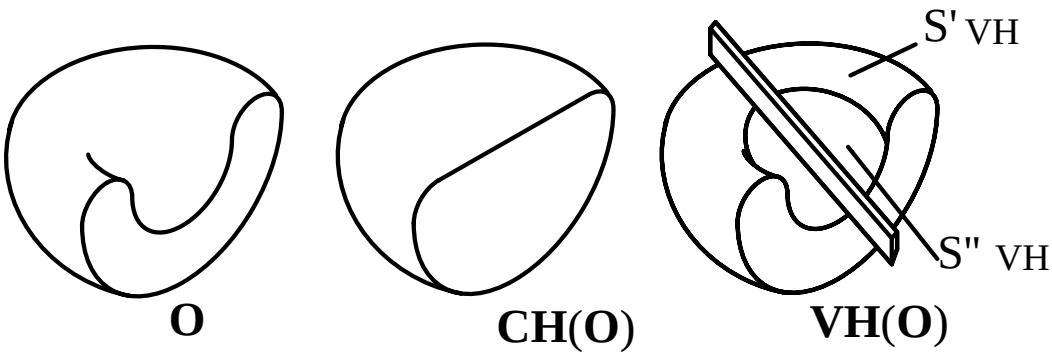

Fig.1. An object **O**, its convex hull **CH**(**O**)and its visual hull VH(O)

Algorithms for computing the visual hulls of polygons, polyhedra and solids of revolution can be found in [9],[10] and [15], to which the reader is referred for further details. Developments and applications of the visual hull idea can be found in [11],[12] and [13].

The basic idea of the aspect graph, introduced in 1979 by Koenderink and van Doorn[8], is clustering the infinite views of an object into a finite set of representative views, or aspects. The views to be clustered are the line drawings obtained by projecting onto the image plane the edges of polyhedra, or the *creases* (surface normal discontinuities) and *limbs* (depth discontinuities) of general objects. The views are clustered into aspects according to their topological structure, and the aspects are arranged into a graph structure, the AG, where each node is labeled with an aspect and each arc represents a topological change, or visual event. The AG is the dual graph of a partition of the viewing space into zones such that all the viewpoints of each zone observe the same aspect.

For perspective AG, each aspect corresponds to a connected open volume of viewpoints, and each visual event to a boundary surface. For the parallel AG, aspects and visual events correspond to open connected areas and boundary lines on the Gaussian sphere. The parallel AG is a sub-graph of the perspective AG. Algorithms for constructing the aspect graphs have been given for polyhedra, articulated objects, solids of revolution and other curved objects under parallel and perspective projection.

For further details the reader is referred to the survey paper [2], to [3], [5], [6], [16]and [17], and to the comprehensive bibliography reported in these papers.

In the following, for computing the visual hull of general smooth curved concave objects, we will use some results presented in [16] by Kriegman, Petitjean and Ponce for computing the aspect graph of the same kind of objects.

The rest of this paper is organized as follows. In Section 2 we relate the surface of the visual hull with two particular boundary surface of the viewing space of the aspect graph. In Section 3 we refine this analysis and determine the cases in which these surfaces can also bound the visual hull. In Section 4 we outline an algorithm for computing the visual hull.

2 VISUAL HULL AND ASPECT GRAPH

In general, the surface S_{VH} of **VH**(**O**) can be divided into two parts: S'_{VH} coincident with the surface S of **O**, and S''_{VH} not coincident with this surface (see Fig.1 for an example). In this section we will relate S''_{VH} to the boundary surfaces of the viewing space corresponding to two particular visual events of the aspect graph of smooth general curved objects. For an exact definition of smooth general curved object, the reader is referred to [16].

A *visual line* relative to an object **O** is a straight line not sharing any point with **O**. The following proposition holds[9].

*Prop.1-A point **p** belongs to **VH(O)** iff no visual line relative to **O** passes trough **p**.*

It follows that:

*Prop.2- A necessary condition for a point **p** to belong to S_{VH} is that there are visual lines relative to **O** arbitrarily close to **p**.*

From these statements we can derive a another necessary condition for a point to belong to the surface of the visual hull S_{VH}.

Prop. 3- A necessary condition for a point ***p*** *to belong to* S_{VH} *is that trough* ***p*** *passes at least one straight line sharing with* ***O*** *only points of its surface S and no point of the interior.*

Proof. By contradiction, let us assume that trough $\mathbf{p} \in S_{VH}$ no such line passes. It follows that any line trough **p** belongs to either of two categories: 1) lines not intersecting **O**; 2) lines sharing with **O** also interior points. If there are lines of the first category, **p** does not belong to **VH**(**O**) because of *Prop.1*. If all the lines passing through **p** belong to the second category, **p** cannot belong to S_{VH} because of *Prop.2* (see Fig. 2, showing a section of **O** made with a plane containing **p**). Thus the hypothesis is contradicted and the proposition proved.

Fig.2. **p** does not belongs to S_{VH} if all lines trough **p** are as L.

Therefore, for finding points of S_{VH} we must consider points of lines sharing some points with the surface S of the object only.

Clearly, if a line L makes contact at only one point **p** with S, only this point belongs to S'_{VH}, since through any other point **p**' of L pass visual lines as L', obtained with an infinitesimal rotation of L about **p**'(see Fig 3).

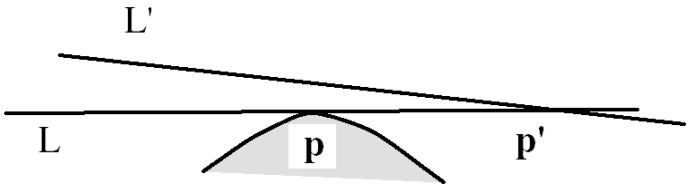

Fig.3. Only **p** belongs to S_{VH}. Trough any other point **p**' pass visual lines as L'.

If a line L makes contact at more then one point with S, and does not share other points with **O**, obviously the contact points belong to S'_{VH}. For the objects bounded by generic smooth curved surfaces considered in this paper, the lines making contact with the object can be tangent at most at three different points [16]. Concluding, for finding S''_{VH} , i.e. the surface of the visual hull not coincident with S, we will analyze lines making two or three contacts with **O**.

2.1. The Case of Bi-tangent Lines

Lines tangent at two different points of S do not yield surfaces but fill volumes, so we need a radical pruning of these lines. For doing this, we will investigate whether the *normals* to S at the tangency points are compatible or not with visual lines passing through points of the tangent line L. This will allow to establish a local necessary condition for a bi-tangent line to contain points belonging to S''_{VH}.

Let us consider a line L tangent at two points $\mathbf{p}_1$ and $\mathbf{p}_2$ of S. Assume different surface normals $\mathbf{n}_1$ and $\mathbf{n}_2$ at $\mathbf{p}_1$ and $\mathbf{p}_2$, and project orthographically these entities along L, together with small segments of the limbs containing $\mathbf{p}_1$ and $\mathbf{p}_2$. Also let P be a plane containing L and **n**, a vector intermediate between $\mathbf{n}_1$ and $\mathbf{n}_2$ (Fig 4(a)) .

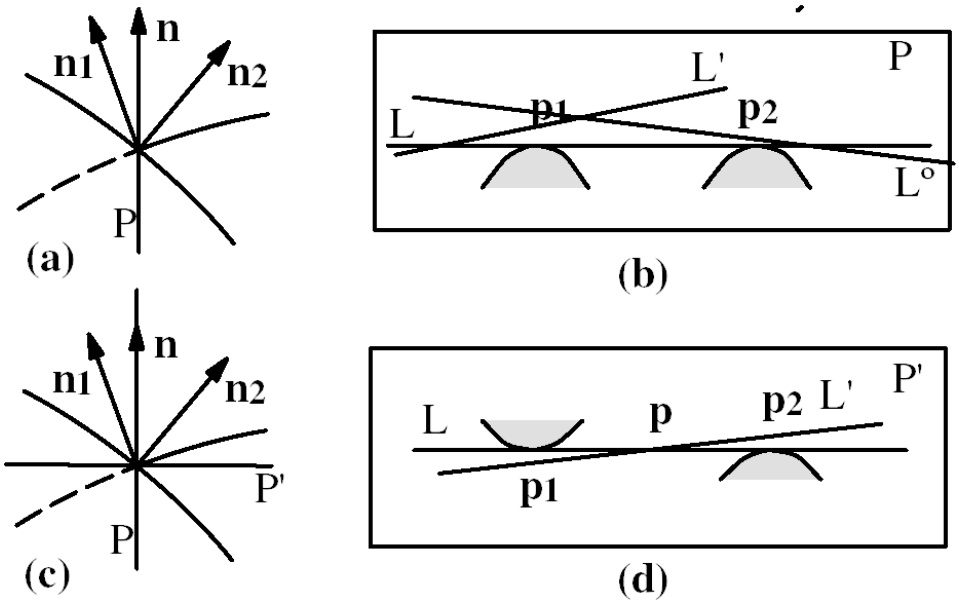

Fig.4- For $\mathbf{n}_1 x \mathbf{n}_2 \neq 0$, no point of L, excluding $\mathbf{p}_1$ and $\mathbf{p}_2$, belongs to S_{VH}

The line L is divided by $\mathbf{p}_1$ and $\mathbf{p}_2$ into two exterior half-open infinite segments and one open interior segment. It is immediately clear that the exterior segments cannot contain points belonging to S''_{VH}, since in the plane P there are visual line as L' and L" in Fig. 4(b), obtained with infinitesimal rotations of L, passing through any point of both segments.

Let us consider the interior segment. In P there are visual lines passing above the segment at an arbitrarily small distance, but no visual lines passes through points of the segment.

The situation changes if we consider visual lines in a plane containing L as P' in Fig.4(c). Its intersection with S is shown in Fig. 4(d). It is clear that through any point **p** of the interior segment passes a visual line as L' compatible with the local geometry.

This shows that, if the vector product $\mathbf{n}_1 x \mathbf{n}_2$ is different from zero, no point of L belongs to S''_{VH}. Thus:

Prop. 4 : a necessary condition for a bi-tangent line to contain points of S''_{VH} is that $\mathbf{n}_1 x \mathbf{n}_2 = 0$, that is $\mathbf{n}_1 = \mathbf{n}_2$ or $\mathbf{n}_1 = -\mathbf{n}_2$.

This result links together visual hull and aspect graphs, since lines of this kind are those which produce the multi-local visual event usually known as *tangent crossing* [4],[6],[7],[16].

For parametric surfaces $\mathbf{p}=\mathbf{p}(u,v)$, the equations which determine the tangency points for these lines are:

$$
\begin{aligned}
&[\mathbf{p}_1(u_1,v_1) - \mathbf{p}_2(u_2,v_2)] \bullet \mathbf{n}_1(u_1,v_1)=0 \\
&[\mathbf{p}_1(u_1,v_1) - \mathbf{p}_2(u_2,v_2)] \bullet \mathbf{n}_2(u_2,v_2)=0 \qquad (1) \\
&[[\mathbf{p}_1(u_1,v_1) - \mathbf{p}_2(u_2,v_2)] x \, \mathbf{n}_1(u_1,v_1)] \bullet \mathbf{n}_2(u_2,v_2)=0
\end{aligned}
$$

where $\bullet$ indicates the dot product, and the surface normals are the vector product of the partial derivatives: $\mathbf{n}(u,v)=\mathbf{n}_u(u,v) x \, \mathbf{n}_u(u,v)$. These are 3 equations in the four variables u_1, v_1, u_2, v_2, and thus determine the curves described by $\mathbf{p}_1$ and $\mathbf{p}_2$ on the surface S. Similar equations can be

written for implicit surfaces (see [13]). A line passing through points $\mathbf{p}_1$ and $\mathbf{p}_2$ determines a ruled boundary surface of the viewing space of the aspect graph which can also bound the visual hull.

2.2 The Case of Tri-tangent Lines

In this case the relationship with the aspect graph is immediately established, since tri-tangent lines produce the visual event known as *triple point* [4],[6],[7],[16].

Also in this case it is easy to write the equations which determine the three tangency points $\mathbf{p}_1$, $\mathbf{p}_2$ and $\mathbf{p}_3$. For parametric surfaces:

$$
\begin{aligned}
&[\mathbf{p}_1(u_1,v_1) - \mathbf{p}_2(u_2,v_2)] \bullet \mathbf{n}_3(u_3,v_3)=0 \\
&[\mathbf{p}_2(u_2,v_2) - \mathbf{p}_3(u_3,v_3)] \bullet \mathbf{n}_2(u_2,v_2)=0 \qquad (2) \\
&[\mathbf{p}_3(u_3,v_3) - \mathbf{p}_1(u_1,v_1)] \bullet \mathbf{n}_1(u_1,v_1)=0 \\
&[\mathbf{p}_1(u_1,v_1) - \mathbf{p}_2(u_2,v_2)] \times [\mathbf{p}_1(u_1,v_1) - \mathbf{p}_3(u_3,v_3)]=0
\end{aligned}
$$

The first three equations state the tangency conditions at $\mathbf{p}_1$, $\mathbf{p}_2$ and $\mathbf{p}_3$. The last equation states that the three points are collinear. The equations for the implicit case can be found in [16]. Since a 3D direction has two degrees of freedom, in the last vector equation only two scalar components are independent. This makes five equations in the six variables u_1, v_1, u_2, v_2, u_3, v_3, which describe three curves on the surface S. Any two of the three points determine the ruled surface which could bound the visual hull.

2.3. Locally Active Lines

Let us summarize the previous results:

Prop.5 - A necessary condition for a point to belong to S''_{VH} *is that it lies on the boundary surfaces of the aspect graph corresponding either to the visual event tangent crossing or to the visual event triple point.*

No other visual event of those catalogued for curved objects (see [4],[6],[7] and[16]) is relevant to the visual hull .

Even though, starting from *Prop.2*, we have been able to work out a stricter conditions for a point to belong to $S"_{VH}$, *Prop.5* is not sufficient for various reasons.

First, for belonging to the surface of the visual hull the bi or tri-tangent lines must not intersect **O**. Second, even if the non-intersection condition is satisfied, a closest analysis of the shape of the surface at the tangency points will show that in several cases the surfaces related to the vial event triple point and tangent crossing cannot bound the visual hull. Furthermore, we will also show that only some segments of the surfaces must be considered as possible boundaries. Finally, these possible boundaries only satisfy *local conditions* at the tangency points: for finding the actual surface of the visual hull from these segments, the algorithm described in Section.4 is required.

We will call *locally active* the lines, the surfaces they form, and their segments which satisfy the more strict local condition that we will derive in the following section.

3. THE LOCALLY ACTIVE SEGMENTS

In this section, we will refine the *local analysis*, i.e. at the tangency points, an find out in which cases segments of lines forming surfaces satisfying *Prop.5* could actually contain points of $S"_{VH}$. This will be done by considering the local constraints due to the shape of S at the tangency points.

For dealing with the local geometry of a smooth surface near a point **p** it will be useful to consider its Gaussian curvature $K(\mathbf{p})$, the product of the principal curvatures $k_1(\mathbf{p})$ and $k_2(\mathbf{p})$. Let us recall that at a point **p** the surface can be approximated by: 1) a paraboloid if $K(\mathbf{p})>0$, 2)a saddle-shaped hyperboloid if $K(\mathbf{p})<0$, 3) a cylinder if $K(\mathbf{p})=0$ and $k_1(\mathbf{p})=0$, or $k_2(\mathbf{p})=0$, but not both [14]. We need not to consider planar points where $k_1(\mathbf{p}) = k_2(\mathbf{p})=0$, since generic surfaces can have only isolated planar points. On a generic surface, points whose Gaussian curvature is strictly positive (*elliptic points*), or strictly negative (*hyperbolic points*), forms open areas separated by curves whose points have zero Gaussian curvature (*parabolic points*)[1],[16].

3.1 Locally Active Segments of Bi-tangent Lines for $n_1 = n_2$

Observe first that only the interior segment of the tangent line could be locally active. This is easily seen by considering the section of **O** made by the plane P_N containing $\mathbf{n}_1$ and $\mathbf{n}_2$. This section is as that shown in Fig.4(b), and the same argument apply. Thus, we must only investigate the interior segment.

For bi-tangent lines we must consider six possible sub-cases, since each tangency point can be elliptic, parabolic or hyperbolic. We will discuss the sub-cases relying, as far as possible, on figures and intuitive geometric reasoning. For each sub-case, the figures show two small areas of S near the tangency points cut by P'_T, a plane parallel to the plane P_T tangent at $\mathbf{p}_1$ and $\mathbf{p}_2$. Each area near $\mathbf{p}_1$ and $\mathbf{p}_2$ is approximated by a paraboloid, a hyperboloid or a cylinder according to the Gaussian curvature. An orthographic projection along L is also shown. The direction of the projectors is always from $\mathbf{p}_2$ to $\mathbf{p}_1$.

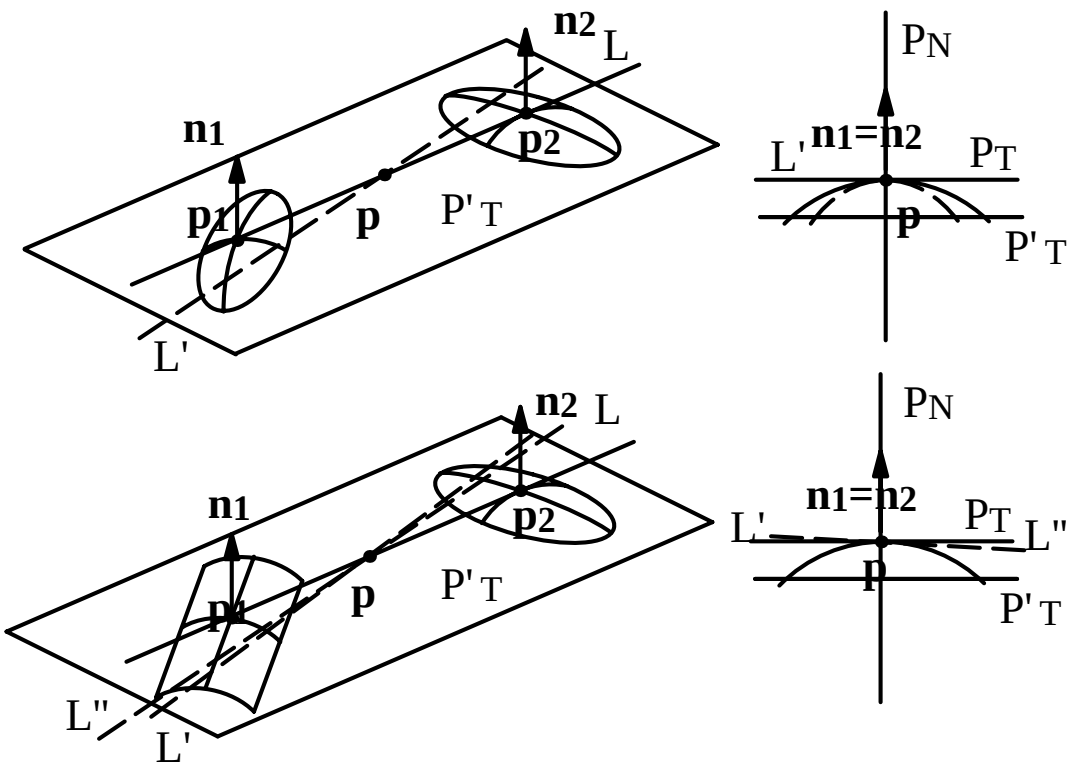

Fig.5. Two inactive sub-cases for bi-tangent lines.

Two inactive sub-cases are shown in Fig.5. Let us consider the first sub-case, concerning two elliptic points. The figure shows that trough any point **p** of the interior segment pass visual lines such as L', obtained with an infinitesimal rotation of L about **p** in P_T. Therefore, the interior segment is not locally active.

The second sub-case of the figure concerns one elliptic point and one parabolic point. A visual line trough any point **p** of the interior segment can be obtained as follows. Rotate again L about **p** in the tangent plane P_T. The line L' obtained will touch S near $\mathbf{p}_1$, the parabolic point. Then perform an infinitesimal rotation of L' about **p** in a plane normal to P_T. This produces the visual line L", and thus also in this case the segment is not locally active.

Three other sub-case cases are shown in Fig.6.

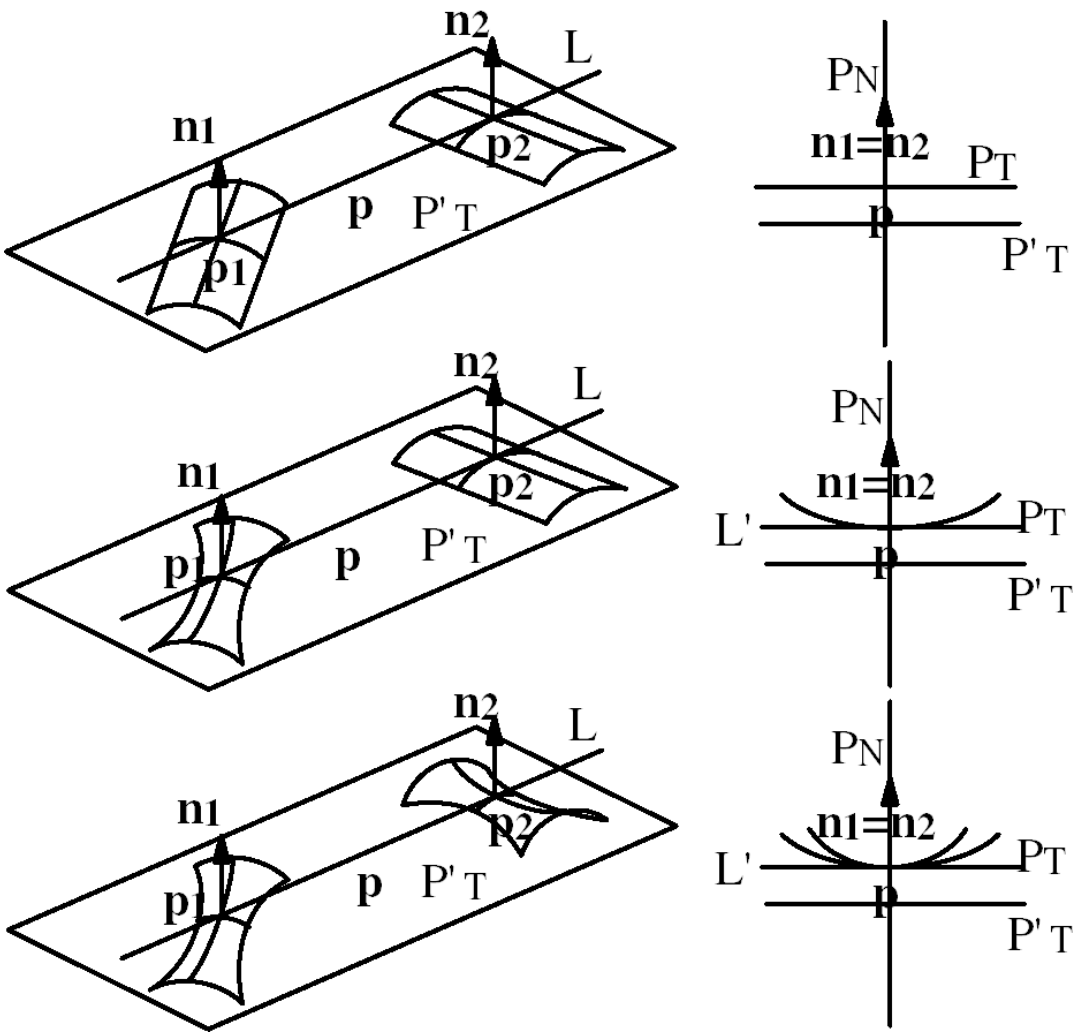

Fig.6. The two bottom sub-cases are locally actives.

Analyzing the first sub-case, concerning two parabolic point, would require considering a more detailed model of the surface, involving derivatives of higher order. However, this is not necessary for our purposes since for generic surfaces this is a limit situation and there are only isolated tangent lines of this kind.

In the two other sub-cases of Fig.6, it is clear that no visual line L' passing through **p** is compatible with the geometry of S near $\mathbf{p}_1$ and $\mathbf{p}_2$.

The sixth sub-case, concerning one elliptic point and one parabolic point, is shown in Fig.7

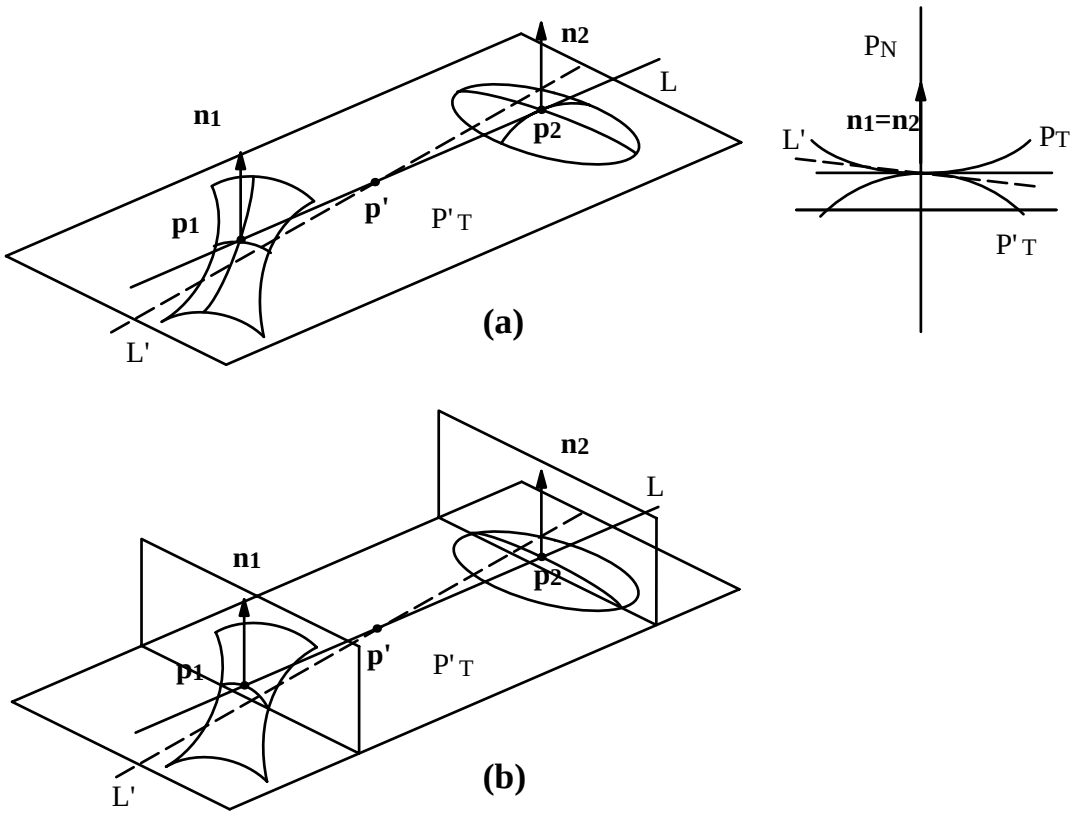

Fig.7. In this case, only a sub-segment near $\mathbf{p}_2$ is locally active

The sub-case cannot be determined by the Gaussian curvatures only. In fact, let us imagine an infinitesimal rotation of L about a point **p** belonging to its interior segment. If the rotated line L' is tangent to S near $\mathbf{p}_1$, the new tangency point will rise above the tangent plane P_T, and correspondingly near $\mathbf{p}_2$ the line L' will lie below P_T. This means that L' could intersect the surface S near $\mathbf{p}_2$. In this case, no visual lines trough **p** are compatible with the local geometry, and **p** belongs to a locally active segment.

The figure allows to understand that this happens for points near $\mathbf{p}_2$, while through points near $\mathbf{p}_1$ can pass visual lines compatible with the local geometry. Then only a sub-segment $\mathbf{p}_2\mathbf{p}$'of the interior segment is locally active. The boundary point **p'** is such that an infinitesimal rotation of L about **p'** is possible such that L' is tangent to S near both $\mathbf{p}_1$ and $\mathbf{p}_2$. For such infinitesimal rotation, the tangency points move along two curves which are the intersections of S and two planes

orthogonal to L at $\mathbf{p}_1$ and $\mathbf{p}_2$ (see Fig.7(b)). It follows that $\mathbf{p}'$ divides the interior segment into two parts such that the ratio of their lengths is equal to the ratio of the radiuses of curvature ρ_1 and ρ_2 of these curves at $\mathbf{p}_1$ and $\mathbf{p}_2$:

$$(|\mathbf{p'}-\mathbf{p}_2|)/(|\mathbf{p'}-\mathbf{p}_1|) = \rho_2/\rho_1$$

The radiuses (actually their inverses, the curvatures) can be computed from the principal curvatures and the direction of L using Euler's theorem[14].

3.2 Locally Active Segments of Bi-tangent Lines for $\mathbf{n}_1 = -\mathbf{n}_2$

Observe first that only the exterior half-open segments can be locally active. This is immediately seen by inspecting the section of **O** made by the plane P_N containing $\mathbf{n}_1$ and $\mathbf{n}_2$ (Fig.8). Visual lines as L' shown in the figure pass through any point of the interior segment.

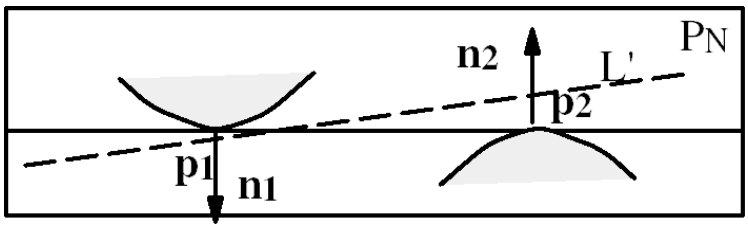

Fig.8- For $\mathbf{n}_1 = -\mathbf{n}_2$, the interior segment is not active

Two inactive sub-cases (two elliptic points; one elliptic and one parabolic point) are illustrated in Fig.9.

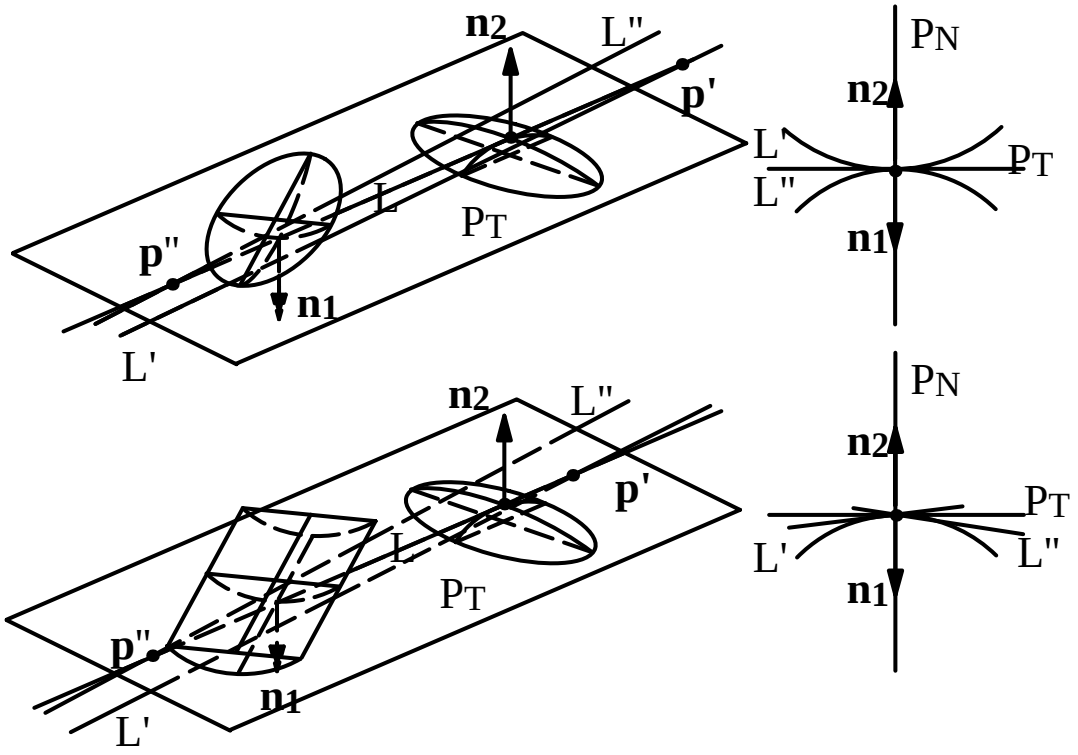

Fig.9. Two inactive sub-cases for $\mathbf{n}_1 = -\mathbf{n}_2$

In the first sub-case, the visual lines L' and L" through points as **p**' and **p**" of the exterior segments are obtained with infinitesimal rotations of L in P_T about these points. In the second sub-case, for obtaining the visual lines two infinitesimal rotations are required, the first in P_T and the second in a plane normal to P_T.

Three other sub-cases are shown in Fig. 10.

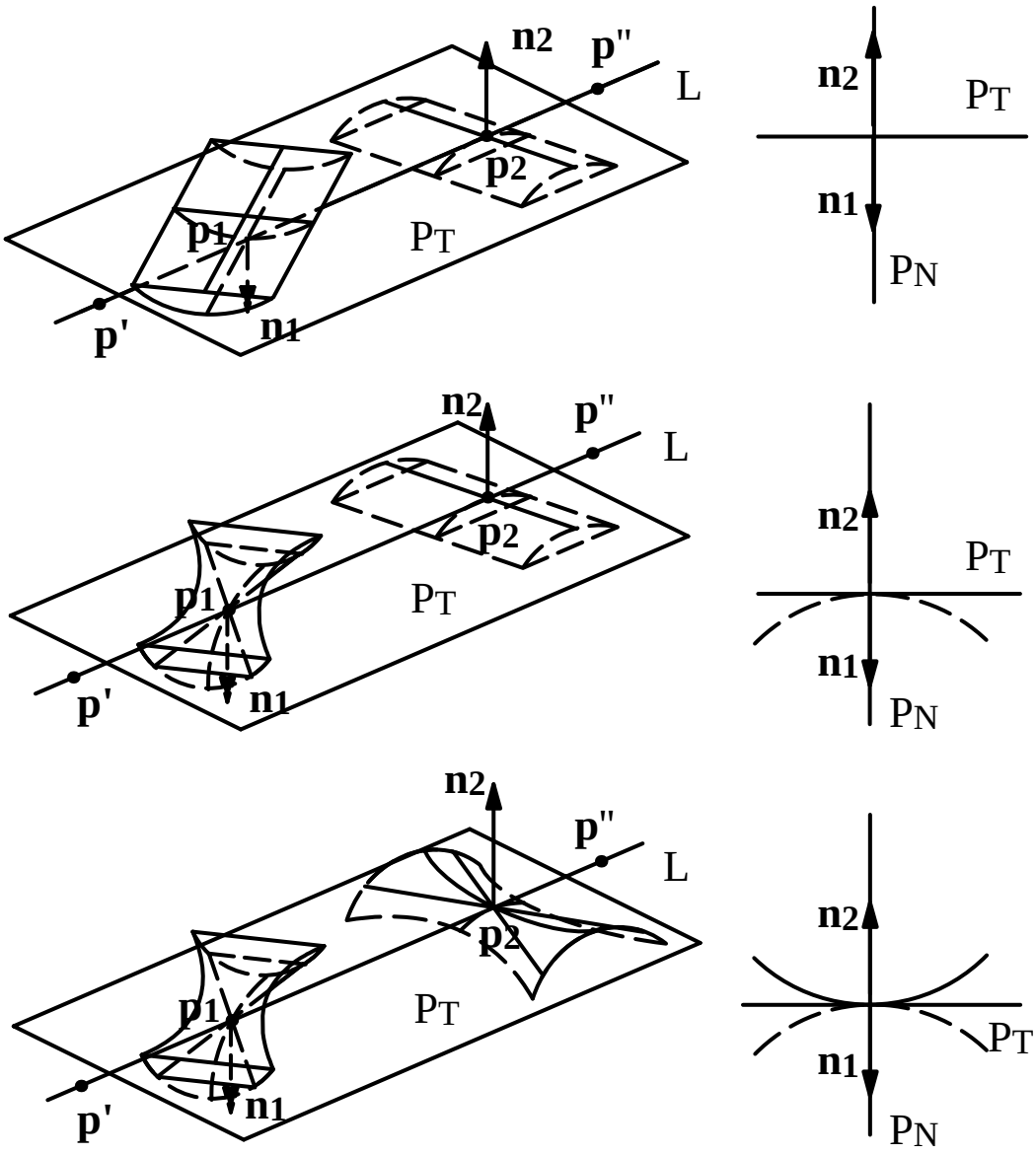

Fig.10. The two bottom sub-cases are locally active.

As for $\mathbf{n_1 = n_2}$, analyzing the sub-case of two parabolic points would require a more detailed model of the surface near $\mathbf{p}_1$ and $\mathbf{p}_2$, but, as before, this is not necessary since we deal with generic surfaces. For the remaining sub-cases, the figure shows that no visual line through points such as **p**' and **p**" is compatible with the local geometry.

The sixth sub-case concerns one elliptic point and one hyperbolic point (Fig.11).

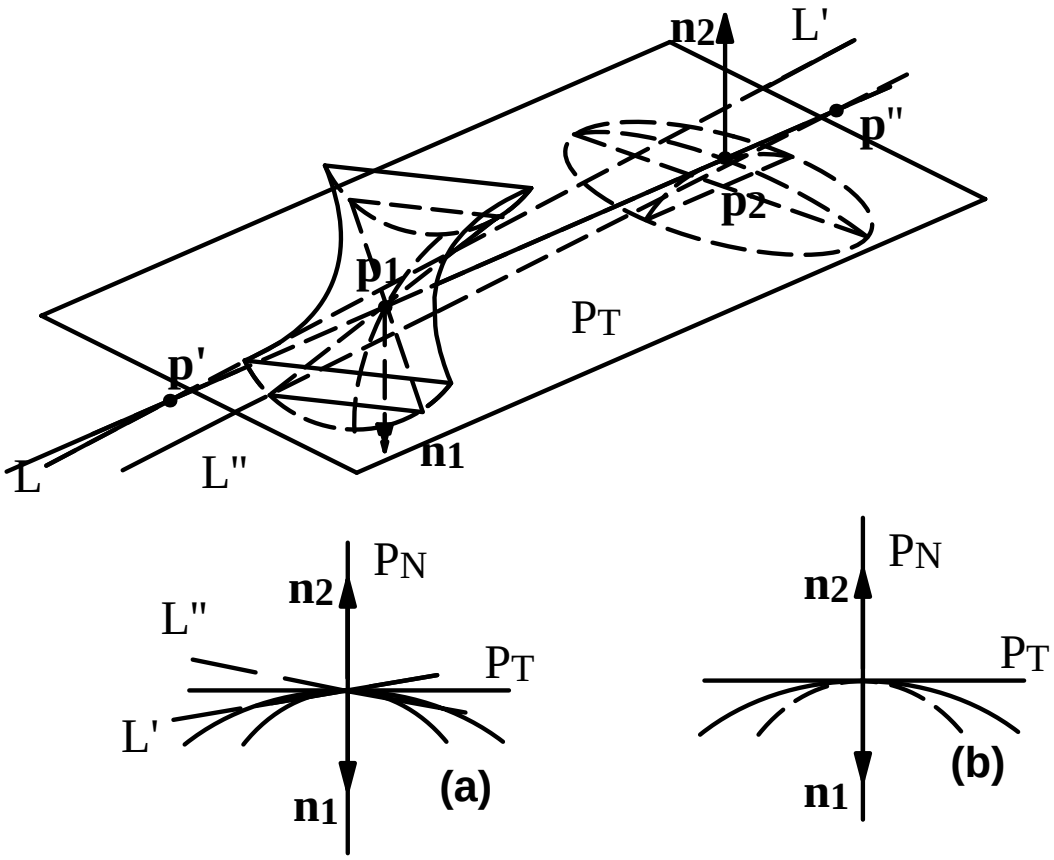

Fig.11. The exterior segments are locally active in case(b).

As in the case of Fig. 7, considering the Gaussian curvature is not sufficient. The figure shows that the exterior segments are locally active depending on the radius of curvature of the curves which are the intersections of S and two planes orthogonal to L at $\mathbf{p}_1$ and $\mathbf{p}_2$. If the radius is smaller for the elliptic point (Fig.11(a)), visual lines as L' and L" through points as **p**' and **p**" are compatible with the local geometry, otherwise the exterior segments are locally active (Fig.11(b)). As for the case in Fig.7, the radiuses are easily computed using Euler's theorem.

3.3. Locally Active Segments of Tri-tangent Lines

Let $\mathbf{p}_1$, $\mathbf{p}_2$ and $\mathbf{p}_3$ be the tangency points of L, and E_1, E_2 and E_3 the orthographic projections along L of infinitesimal segments of the limbs containing $\mathbf{p}_1$, $\mathbf{p}_2$ and $\mathbf{p}_3$.

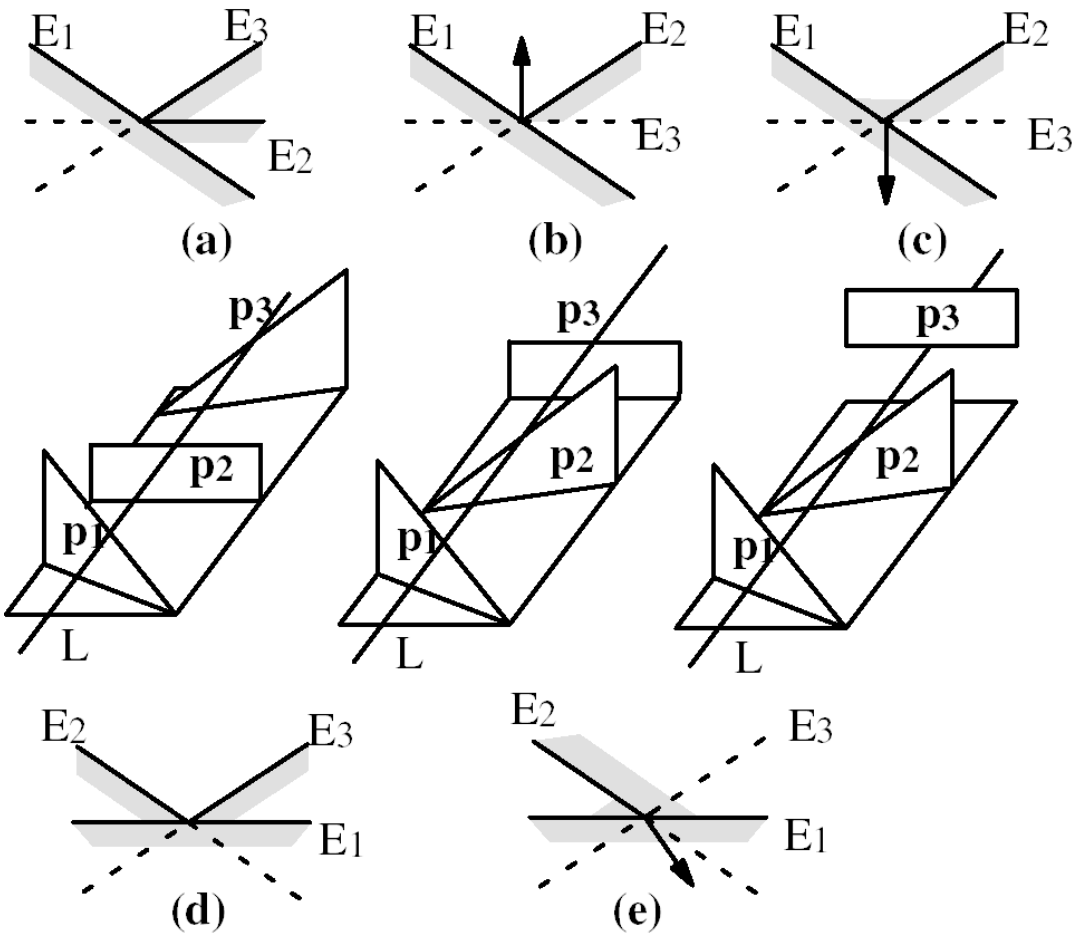

Fig.12. The possible arrangements of the limbs for tri-tangent lines

Three spatial arrangements of the limbs, shown in Fig.12. (a), (b) and (c), are possible. For each case the figure shows the orthographic projection along L and an assonometric view. In the orthographic projection the arrow, pointing outside the object, marks a limb covered by the others. Inspecting the orthographic projections could suggest that two other cases exist, shown in Fig.12 (d) and (e). Actually, cases (d) and (e) are cases (b) and (c) observed from the opposite side. Case (a) produces the same projections from both sides.

The tri-tangent line L is divided into two interior open segments and two half-open exterior segments. In order to determine the locally active segments, for each case we will consider the possible visual lines passing through points of L and lying in a plane P_R rotating about L. The trace

of P_R in the orthographic projection plane can lie in three different areas, as shown for case (a) in Fig.13 (a), where the areas are marked 1, 2 and 3.

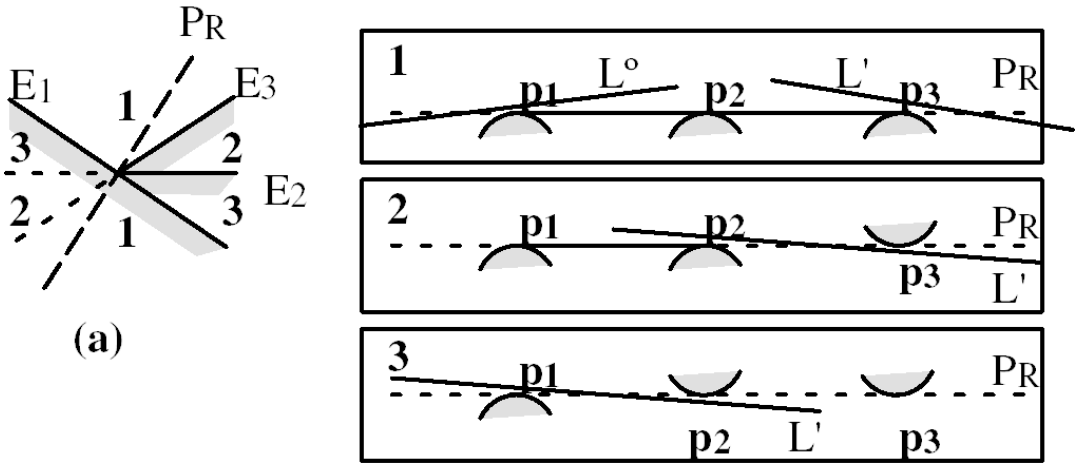

Fig.13. Arrangement (a) does not yield active segments

The figure also shows, for case (a), the three possible intersections of P_R and S. The first intersection shows that the exterior segments are inactive, since small rotations of L about any point of these segments produce visual lines as L' and L''. Intersections 2 and 3 show that also the interior segments are inactive. Concluding, case (a) does not produce active segments.

We omit for brevity a similar analysis for cases (b) and (c). The results obtained are summarized in Fig.14 , where the locally active segments of tri-tangent lines are solid.

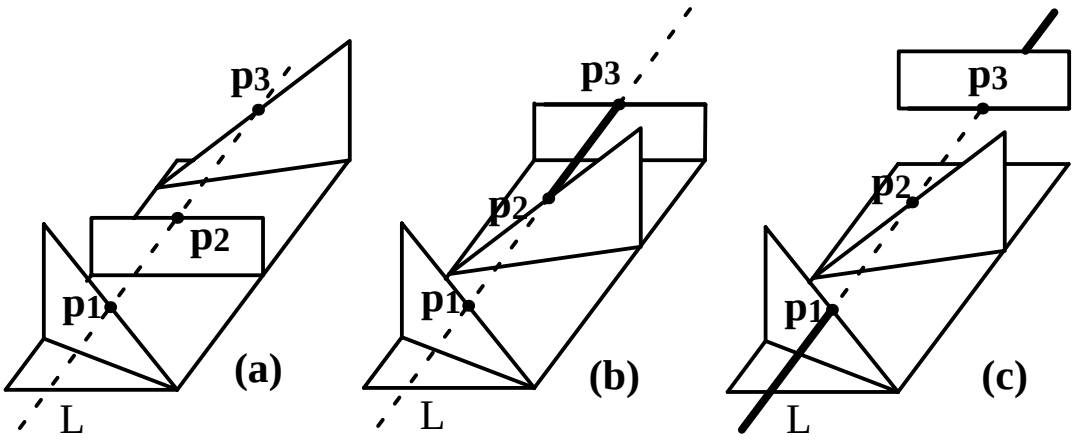

Fig.14-The locally active segments of tri-tangent lines.

4. AN ALGORITHM FOR COMPUTING THE VISUAL HULL

In this section we outline an algorithm for computing the visual hull of a smooth curved object. The algorithm exploits some parts of the algorithm implemented by Kriegman, Petitjean and Ponce[16] for computing the aspect graph of smooth curved objects .

Step 1- The techniques described in [16] for solving the systems (1) and (2), or the equivalent systems for implicit surfaces, can be used for obtaining the pairs $\mathbf{p}_1$ and $\mathbf{p}_2$ for the visual event tangent crossing, and the triplets $\mathbf{p}_1$, $\mathbf{p}_2$ and $\mathbf{p}_3$ for the visual event triple point. These points form curves on the surface S, and the tangent line L produces ruled surfaces.

Step 2- We discard the curves, or their parts, related to tangent lines which:

1) do not satisfy the local necessary conditions determined in Section 3;
2) intersect S.

We also discard the parts of ruled surfaces not locally active, and obtain a set of locally active patches, each with an exterior side (where visual lines compatible with the tangency points pass).

Step 3- A possible approach to computing S_{VH} from the curves and surfaces determined in the previous step the is as follows.

Let us determine first S'_{VH}. The surface S is divided by the curves not discarded into a number of areas. Each area entirely belongs or not to S'_{VH}. For each area we chose a random point $\mathbf{p}$, determine the plane P_T tangent to S at $\mathbf{p}$, and intersect P_T and S. Let C be the intersection curve. If:

a) C reduces to $\mathbf{p}$

or

b) there exist in P_T at least one line tangent to C without intersecting C

there are visual lines passing at an arbitrarily small distance from **p**, and therefore the whole area belongs to S'_{VH}.

By applying this procedure to all areas of S, we obtain S'_{VH} and a number of areas (possibly none) consisting of concavities not belonging to S'_{VH}. For each such area there is a boundary curve, consisting of one or more segments. At each segment starts a locally active patch, which belongs to S''_{VH} until it touches S again, or is intersected by another locally active patch. In the latter case, we must add to S''_{VH} the part of the new patch which lies on the interior side of the old patch. This procedure is iterated until the entire area is covered.

It must be observed that the technique of Step 3, consisting in covering the concavities with locally active patches, could fail to determine the entire visual hull of multiply connected objects. In fact, a multiply connected object **O** could have a visual hull with some parts not connected to **O**[9], which are not detected by the technique of Step.3.

A general volumetric approach, working for any smooth object, consists in constructing the partition of $\boldsymbol{R}^3$ generated by all the locally active patches. Each cell of this partition belongs entirely or not to the visual hull, and the whole visual hull can be constructed by checking each cell and merging together those belonging to the visual hull. To check a cell, chose a random point in it, and construct the cone formed by the lines passing through the point and tangent to **O**. The cell belongs to the visual hull if all the tangent lines also intersect **O**.

5. CONCLUSIONS

In this paper we have developed the theory of the visual hull of smooth curved objects. A main result is the link established between the visual hull and the aspect graph of these objects. We have shown that S''_{VH}, the surface of the visual hull not coincident with the surface S of the original object, consists of patches of the boundary surfaces of the viewing space of the aspect

graph. These surfaces correspond to the visual events tangent crossing and triple point of smooth curved objects.

We have also shown that only in some cases patches of these surface can bound the visual hull, and we have determined these cases by inspecting the geometry of the surface S at the tangency points. We have also outlined an algorithm for computing the visual hull, which in part exploits an algorithm implemented for computing the aspect graph. Future work will be aimed at implementing this algorithm.

6. REFERENCES

[1] V.I.Arnold, *Catastrophe Theory,* Springer-Verlag, Heidelberg,1984

[2] K.W. Bowyer and C.R. Dyer, "Aspect Graphs: An Introduction and Survey of Recent Results," *Int'l J. Imaging Systems and Technology*, vol.2, pp. 315-328, 1990

[3] K.Bowyer , M. Sallam, D.Eggert and J. Stewman, "Computing the Generalized Aspect Graph for Objects with Moving Parts," *IEEE Trans. Pattern Analysis and Machine Intelligence*, vol.15, no.6, pp.605-610, 1993

[4] J.Callahan and R. Weiss,"A Model for Describing Surface Shape," in *Proc. IEEE Conf. on Comp. Vision and Pattern Recognition,* pp. 240-245, 1985

[5] D.W. Eggert , K.W. Bowyer, C.R. Dyer, H.I. Christensen, and D.B. Goldof, "The Scale Space Aspect Graph, "*IEEE Trans. Pattern Analysis and Machine Intelligence*, vol.15, no.11, pp.1,114-1139, 1993

[6] D.Eggert and K.Bowyer," Computing the Perspective Aspect Graph of Solids of Revolution,"*IEEE Trans. Pattern Analysis and Machine Intelligence*, vol.15, no.2, pp.109-128, 1993

[7] Y.K. Kergosien,"La Famille des Projections Orthogonales d'Une Surface et Ses Singularités," *C.R. Acad.Sc.Paris,* 292, pp.929-932, 1981

[8] J. J.Koenderink and A. J. van Doorn," The Internal Representation of Solid Shapes with Respect to Vision," *Biol. Cybern*. vol.32, pp.211-216, 1979

[9] A. Laurentini," The Visual Hull Concept for Silhouette-based Image Understanding,*"* *IEEE Trans. Pattern Analysis and Machine Intelligence,*vol.16, pp.150-162, 199

[10] A. Laurentini, "Computing the Visual Hull of Solids of Revolution," *Pattern Recognition*, vol. 32, pp.377-388, 1999

[11] A. Laurentini ," How Far 3-D Shapes Can Be Understood from 2-D Silhouettes," *IEEE Trans. Pattern Analysis and Machine Intelligence,* vol. 17, pp.188-195, 1995

[12] A. Laurentini, "Surface Reconstruction Accuracy for Active Volume Intersection," *Pattern Recognition Letters*, vol. 17, pp. 1285-1292, 1996

[13] A. Laurentini," How Many 2D Silhouettes it Takes to Reconstruct a 3D Object," *Comput. Vision and Image Understanding,* vol.67, pp. 81-87, 1997

[14] B.O'Neill, *Elementary Differential Geometry*, Academic Press, San Diego, 1996

[15] S. Petitjean,"A Computational Geometric Approach to Visual Hull," *Int. J. of Comput. Geometry and Appl*., vol. 8, no.4, pp. 407-436, 1998

[16] S.Petitjean, J.Ponce and D.J.Kriegman, "Computing exact aspect graphs of curved objects: algebraic surfaces," *Int'l J. of Computer Vision*, vol. 9, no.3, pp.231-255, 1992

[17] I. Shimshoni and J.Ponce, "Finite Resolution Aspect Graphs of Polyhedral Objects," *IEEE Trans. Pattern Analysis and Machine Intelligence,* vol.19, no.4, pp.315-327, 1997